Cellular and Molecular Life Sciences (2019) 76:3449–3464
https://doi.org/10.1007/s00018-019-03081-w

ORIGINAL ARTICLE

Ascorbate inducible N259 glycans on prolyl 4-hydroxylase subunit α1 promote hydroxylation and secretion of type I collagen

Run Shi[1,2,3] · Weimin Hu[3] · Yan Zhang[1] · Shanshan Gao[1] · Andrew H. Smith[4,5] · Jun Ye[6] · Lili Cai[1] · Linda M. Graham[4,5] · Chaoyang Li[1,3]

Received: 8 October 2018 / Revised: 19 March 2019 / Accepted: 20 March 2019 / Published online: 27 March 2019

Abstract

Ascorbic acid (vitamin C, VC) increases the secretion of mature collagen by promoting the activity of prolyl 4-hydroxylase subunit α 1 (P4HA1). To explore the mechanism involved, we investigated the role of N-linked glycosylation, which can regulate enzyme activity. P4HA1 has two glycosylation sites, Asn (N) 113 and N259. Our studies show that glycosylation of N259, but not N113, by STT3B and magnesium transporter 1 (MAGT1) is augmented by VC. N259 glycosylation on P4HA1 correlates with enhanced pepsin-resistant collagen 1α2 secretion. Downregulation of *Stt3b* and *Magt1* reduces N259 glycans on P4HA1. In collagen 1α2 purified from *Stt3b*-silenced fibroblasts, decreased hydroxylation is found at five specific proline residues, while significantly increased hydroxylation is noted at two proline residues. Similarly, in collagen 1α1, reduced proline hydroxylation is detected at eight sites and increased proline hydroxylation is found at four sites. These results suggest that N-linked glycosylation of P4HA1 can direct hydroxylation at specific proline residues and affect collagen maturation.

Keywords Ascorbic acid · Type I collagen · Prolyl 4-hydroxylase · Post-translational modification · STT3B · MAGT1 · N-glycosylation

Introduction

Collagen is the main component of connective tissues in animals and comprises of 25–35% of the body's protein content. Collagens can be separated into fibrillar and non-fibrillar groups, fibrillar being the most abundant, and type I collagen being the main fibrillar collagen. Biosynthesis of type I collagen requires several steps [1]. After preprocollagen is translated on the ribosomes along the rough endoplasmic reticulum (RER), the N-terminal signal is cleaved in the lumen of the RER to form procollagen. In the RER, proline and lysine are hydroxylated by prolyl and lysyl hydroxylases, for which ascorbic acid (vitamin C, VC) is a co-factor. The hydroxylation of proline and lysine is essential for collagen maturation [2]. Specific hydroxylysine residues are glycosylated promoting the formation of the mature collagen triple helix that is pepsin-resistant. This triple helix is then transported to Golgi apparatus to be secreted.

Proline is hydroxylated by one or more of three isoforms of prolyl hydroxylase (P4H), P4HA1, P4HA2, and P4HA3 [3–6], all of which use VC as a co-factor. Besides P4H, lysyl hydroxylase (Procollagen-Lysine, 2-Oxoglutarate 5-Dioxygenase, PLOD) also uses VC as a co-factor [7, 8]. Deficiency

Electronic supplementary material The online version of this article (https://doi.org/10.1007/s00018-019-03081-w) contains supplementary material, which is available to authorized users.

✉ Linda M. Graham
grahaml@ccf.org

✉ Chaoyang Li
cyli@wh.iov.cn

1 State Key Laboratory of Virology, Wuhan Institute of Virology, Chinese Academy of Sciences, 44 Xiao Hong Shan Zhong Qu, Wuhan 430071, Hubei, China

2 University of Chinese Academy of Sciences, Beijing, China

3 Affiliated Cancer Hospital and Institute of Guangzhou Medical University, 78 Heng Zhi Gang Road, Guangzhou 510095, China

4 Department of Biomedical Engineering, Lerner Research Institute, Cleveland, OH, USA

5 Department of Vascular Surgery, Cleveland Clinic, Cleveland, OH, USA

6 Department of Statistics, University of Akron, Akron, OH, USA

of VC compromises P4H and PLOD activity, resulting in decreased hydroxylation of collagen leading to the disease condition known as scurvy. Although P4H activity has been reported to be regulated by short-term treatment with VC [9, 10], the mechanism of enzymatic activity regulation is not completely understood.

N-linked glycosylation is one of the most common forms of post-translational modification, and serves to facilitate protein folding, solubility, and stability, and to regulate the function and activity of multiple enzymes [11].Glycosylation of P4HA1 has been reported [12]; however, the function of the N-glycosylation of P4HA1 remains unclear. In fact, the enzymatic activity of P4HA1 is reported to be unaffected by the lack of glycans [12, 13].

Since VC is required for collagen maturation, we sought to better understand the role of VC in collagen production, particularly the mechanism by which VC and P4H accelerate collagen maturation. We report that treatment of fibroblasts for 3–6 h (hours) with VC increases the secretion of mature collagen 1α2 (col 1α2) by increasing P4HA1 glycosylation, specifically at N259. N259 glycosylation induces P4HA1 to hydroxylate specific prolines in col 1α2, resulting in more pepsin-resistant collagen. Silencing STT3B or magnesium transporter 1 (MAGT1), the enzymes responsible for N259 glycosylation on P4HA1, significantly decreases hydroxylation of five prolines in col 1α2 and eight prolines in col 1α1. On the other hand, a significant increase in hydroxylation of two prolines in col 1α2 and four prolines in col 1α1 is detected.

Results

Short-term VC treatment increased col1α2 secretion

VC treatment stimulated proline or lysine hydroxylation and increased secretion of mature Type I collagen [9, 10], which is a triple-stranded helix composed of two α1(I) chains and one α2(I) chain. We verified the effect of VC on Type I collagen secretion on mouse embryonic fibroblast (MEF) cells, human foreskin fibroblast (HFF) cells, and human embryonic lung fibroblast (HEL) cells with 50 μM VC. Two bands were detected by immunoblot analysis 3 h after treatment (Fig. 1a–c, top panel; supplemental Fig. 1A). By silencing *Col1a2* and producing an antibody specific for col 1α1, we determined that the protein with an apparent molecular weight of 150 kDa was col 1α2 and the 200 kDa protein is col 1α1 (Supplemental Fig. 1A). Since both proteins showed similar pattern after VC treatment, we focused our study on col 1α2, because the antibody is commercially available.

VC treatment enhanced collagen secretion in skin fibroblasts [10], and we verified that 6 h of VC treatment significantly increased col 1α2 in the culture medium and reduced col 1α2 in the cell lysate of MEF, HFF, and HEL cells(Fig. 1a–c, middle and bottom panels, $n=3$). Interestingly, VC treatment did not increase *Col1a2* mRNA. Actinomycin D, a transcription inhibitor, did not reduce the short-term effect of VC (Supplemental Fig. 2B, $n=3$). Thus, a short period of VC treatment did not enhance *Col1a2* mRNA transcription, but increased col 1α2 secretion of pepsin-resistant collagen (Supplemental Fig. 2C & 2D).

Prolyl hydroxylase was responsible for VC-stimulated col 1α2 secretion

Proline and lysine hydroxylation by P4H and PLOD, respectively, are important for collagen triple helix formation, which has increased pepsin resistance and secretion rate [14–17]. To determine if VC activates proline or lysine hydroxylases, MEF cells were treated with ethyl-3,4-dihydroxybenzoate (EDBH), a prolyl hydroxylase inhibitor, or minoxidil, an inhibitor of lysyl hydroxylase transcription. EDBH, but not minoxidil, treatment resulted in significant retention of col 1α2 in the cell, reduced col 1α2 secretion, and decreased pepsin-resistant collagen in the culture medium (Supplemental Fig. 3A & 3B, $n=4$). These results suggested that induction of one or more of the P4H isoforms accounted for the increased col 1α2 secretion.

P4HA1 enhanced pepsin-resistant col 1α2 secretion in MEF cells treated with VC

Three isoforms of P4H have been shown to hydroxylate proline in collagen. P4HA1 and P4HA2 were expressed in MEF cells (Supplemental Fig. 4A). Expression of P4HA3, which is found primarily in cancer cells [6], was not assessed due to lack of a commercially available antibody for mouse P4HA3. Silencing *P4ha1* in MEF cells with shRNAi did not affect protein or mRNA levels of *P4ha2* (Fig. 2a, left and middle panels), and did not impact the mRNA levels of *Col 1a2* (Fig. 2a, left panel). The amount of VC-stimulated pepsin-resistant col 1α2 in culture medium, however, was significantly decreased (Fig. 2a, right and middle bottom panels). Knocking out *P4ha2* in MEF cells did not impact the P4HA1 expression or the amount of pepsin-resistant col 1α2 in the medium (Fig. 2b). Thus, silencing *P4ha1*, but not *P4ha2*, significantly impacted col 1α2 secretion, indicating that P4HA1 is one of the isoforms responsible for VC-induced proline hydroxylation on col 1α2.

Silencing *P4ha1* could result in reduced col 1α2 protein stability. To determine the effect on protein stability, control and *P4ha1* shRNAi transfected MEF cells were incubated with 100 μg/ml cycloheximide (CHX) and intracellular collagen was measured from 0 to 2.5 h. Immunoblot analysis showed no detectable collagen secretion during this time

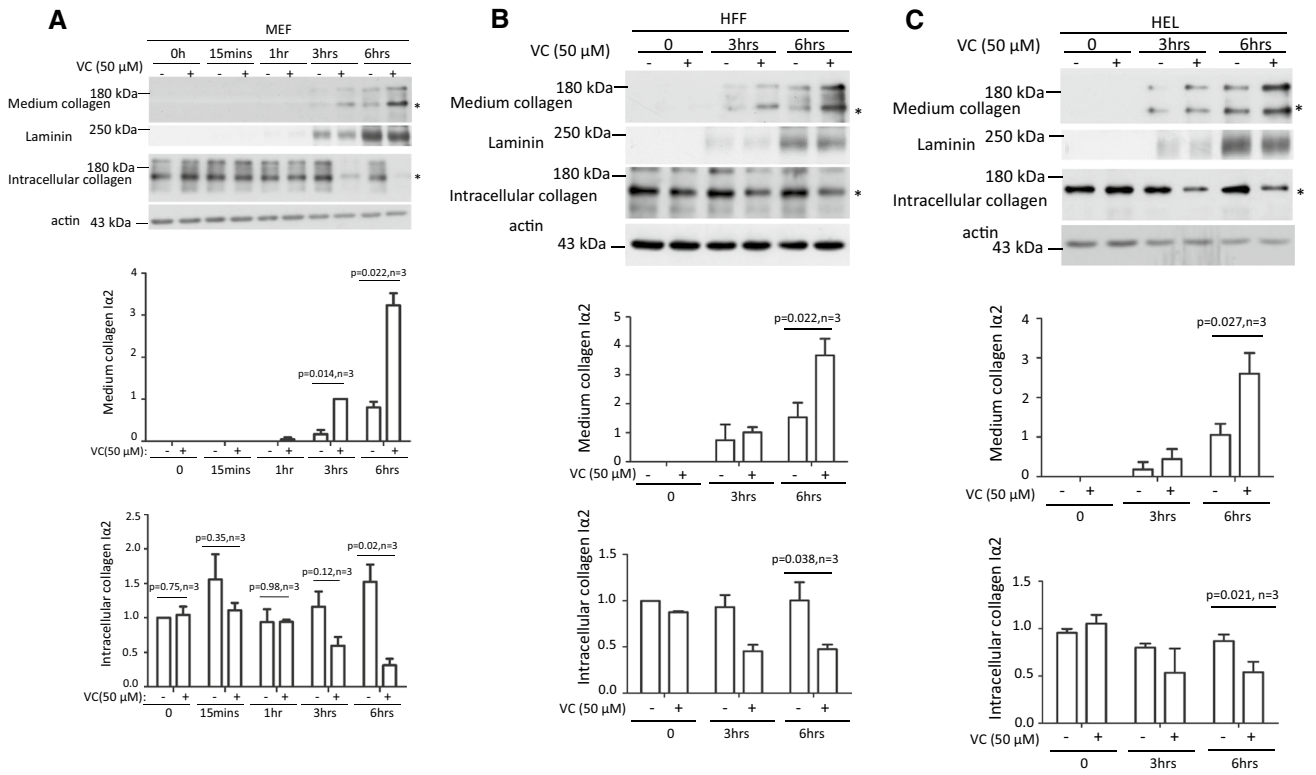

Fig. 1 Short-term VC treatment enhanced pepsin-resistant col1α2 secretion via a pathway independent of transcription. Time course of MEF cells (**a**), HFF cells (**b**), and HEL cells (**c**) treated with 50 μM of VC showed that more col 1α2 could be detected in the culture medium compared to non-treated cells. A consistent difference was first detected 3 h post-treatment of MEF cells (**a**: middle panel, $n=3$). By 3 h after treatment, less intracellular col 1α2 was detected in VC-treated cells compared with non-treated cells (**a**: bottom panel, $n=3$). A consistent difference was detected 6 h after treatment of HFF and HEL cells (**b**, **c**: middle panel, $n=3$). Significantly less intracellular col 1α2 could be detected in VC-treated cells compared with non-treated cells at 6 h after treatment (**b**, **c**: bottom panel, $n=3$). Laminin was used as a loading control for culture medium protein. Actin was used as a loading control for cell lysate protein. Asterisk indicates the position of col 1α2. Immunoblot densitometry was quantified using Image J and depicted graphically

course (data not shown). No significant differences in the rate of intracellular collagen degradation were observed between control and *P4ha1* silenced MEF cells (Fig. 2c, $n=3$). These results indicated that silencing *P4ha1* did not reduce col 1α2 stability. In addition, no significant difference in col 1α2 stability in culture media was detected with *P4ha1*-silenced or control MEF cells after VC treatment (Fig. 2d, $n=3$).

Short-term VC treatment stimulated N259 glycosylation on P4HA1

During the preceding studies, it was noted that the P4HA1 antibody recognized an additional protein band in VC-treated MEF cells that was not present in untreated cells (Fig. 2a). This suggested that VC treatment caused a post-translational modification of P4HA1. In MEF cells treated with varying concentrations of VC for 6 h, a dose-dependent appearance of this additional protein band was noted with obvious effect at 40 μM of VC (Fig. 3a). This presumed post-translational modification of P4HA1 was also detected in HEL and HFF cells treated with 40 μM VC (Fig. 3b), raising the possibility that the conserved post-translational modification induced by short-term VC treatment might modulate the activity of the enzyme.

N-linked glycosylation of P4HA1 has been reported [18], suggesting that the additional protein band induced by VC treatment could represent a glycosylated P4HA1 protein. Therefore, MEF cell lysates were treated with peptide-N-glycosidase F (PNGase F) to remove N-linked oligosaccharides. This abrogated the double-band pattern induced by VC treatment and resulted in a single band with enhanced electrophoretic mobility (Fig. 3c). These results suggested that P4HA1 undergoes constitutive N-linked glycosylation, and may be further modified by additional N-linked glycans in response to short-term VC treatment.

Since N113 and N259 (based on numbering from the N-terminus of the immature protein) are the two known glycosylation sites on P4HA1, we investigated which glycosylation site was affected by VC. N113Q, N259Q,

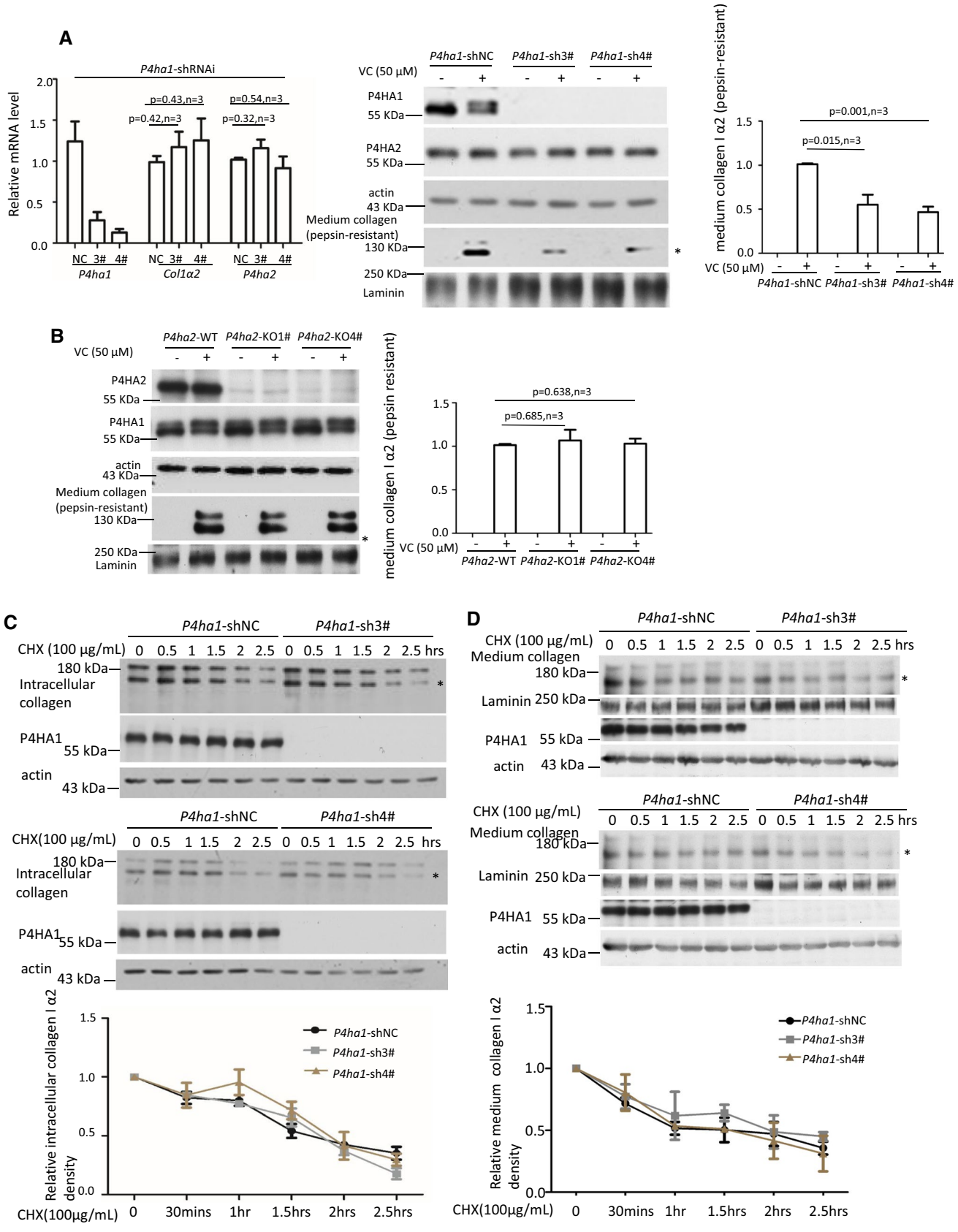
A
P4ha1-shRNAi
Relative mRNA level
p=0.43,n=3
p=0.54,n=3
p=0.42,n=3
p=0.32,n=3
NC 3# 4#
P4ha1
Col1α2
P4ha2
VC (50 μM)
P4ha1-shNC
P4ha1-sh3#
P4ha1-sh4#
P4HA1
55 KDa
P4HA2
actin
43 KDa
Medium collagen
(pepsin-resistant)
130 KDa
250 KDa
Laminin
medium collagen I α2 (pepsin-resistant)
p=0.001,n=3
p=0.015,n=3
B
P4ha2-WT
P4ha2-KO1#
P4ha2-KO4#
p=0.638,n=3
p=0.685,n=3
C
CHX (100 μg/mL)
0 0.5 1 1.5 2 2.5 hrs
Intracellular
collagen
180 kDa
P4HA1
55 kDa
actin
43 kDa
Relative intracellular collagen I α2
density
CHX(100μg/mL)
0 30mins 1hr 1.5hrs 2hrs 2.5hrs
D
Medium collagen
Laminin 250 kDa
Relative medium collagen I α2
density

◂**Fig. 2** P4HA1 contributed to VC-enhanced col 1α2 secretion. **a** qPCR showed that silencing of *P4ha1* did not affect the expression of *Col1a2* and *P4ha2* mRNA but significantly reduced pepsin-resistant col 1α2 in the culture medium. P4HA1, P4HA2, or Col 1A2 mRNA or protein was detected with quantitative PCR or immunoblotting, respectively. NC: *P4ha1*-shRNAi-negative control; 3#: *P4ha1*-shRNAi-3#; 4#: *P4ha1*-shRNAi-4# ($n=3$) (left panel). **b** Knockout of *P4ha2* did not impact P4HA1 protein level, its glycosylation, or pepsin-resistant col 1α2. Downregulation of *P4ha1* did not reduce the stability of intracellular col 1α2 (**c**) and secreted col 1α2 (**d**). 50 μM of VC-treated *P4ha1*-silenced or control cells were treated with 100 μg/mL CHX for varying times and cell lysates or culture media were immunoblotted for col 1α2 (**c** panels 1 and 4 for intracellular collagen stability; **d** panels 1 and 5 for stability of collagen in culture media). Wherever possible, Laminin was used as a loading control for culture medium protein, whereas actin was used as a loading control for cell lysate protein. Densitometry of cell lysate col 1α2 or secreted col 1α2 was quantitated using image J and depicted graphically ($n=3$, $p=$NS). Asterisk indicates col 1α2

and N113Q/N259Q P4HA1 mutants were generated, and plasmids were separately transfected into *P4ha1*-silenced MEF cells. Interestingly, while electrophoretic mobility of influenza hemagglutinin epitope (HA) tagged wild-type (WT) P4HA1 and HA-tagged N259Q P4HA1 was identical in the absence of VC treatment, mobility of the N113Q P4HA1 and N113Q/N259Q P4HA1 was increased equally (Fig. 3d). Treatment with PNGase F demonstrated that differences in the electrophoretic mobility of HA-tagged P4HA1 were due to differences in the degree of N-linked glycosylation (Fig. 3d). These results suggested that N113 glycosylation occurs constitutively in the absence of VC treatment. To prove that N113 glycosylation was VC treatment independent, we treated MEF cells bearing N259Q mutated P4HA1 with or without VC for 6 h. We found that the migration of N259Q mutated P4HA1 was not affected by VC treatment (Fig. 3e, top panels). In addition, when the cell lysates were subjected to PNGaseF treatment, the mobility of the protein was consistently enhanced compared to cell lysate without PNGaseF treatment (Fig. 3e, bottom panels). Thus, N113 was glycosylated, but the glycosylation was not induced by VC treatment.

To show that N259 glycosylation depended on VC treatment, *P4ha1*-silenced MEF cells were transfected with the N113Q P4HA1 mutant and treated with VC for 6 h. Enhanced N259 glycosylation of P4HA1 was induced by VC (Fig. 3f, top panel), although with apparently lower efficiency than in WT MEF cells (compare Fig. 3a, f, top panel). When those cell lysates were treated with or without PNGaseF, the higher molecular weight band disappeared, but the bottom band remained, suggesting that it was resistant to PNGaseF treatment (Fig. 3f, bottom panel). Thus, N259 glycosylation of P4HA1 is induced by VC treatment.

N259 glycosylation on P4HA1 was post-translationally modified by STT3B/MAGT1 complex upon VC treatment

N-linked glycosylation can be co-translational or post-translational. Co-translational N-linked glycosylation depends on STT3A, whereas post-translational N-linked modification depends on STT3B/MAGT1 complex [19]. To investigate the nature of N113 and N259 glycosylation, we silenced *Stt3a* or *Stt3b* separately in MEF cells (Fig. 4a, b). Silencing *Stt3a* or *Stt3b* did not reduce P4HA1 protein and did not result in glycan-deficient P4HA1 in untreated cells (Fig. 4a, b). Thus, STT3A or STT3B did not affect N113 glycosylation on P4HA1. In addition, silencing *Stt3a* neither reduced N259 glycosylation induced by VC nor impacted the mRNA level of *Stt3b* (Fig. 4a). These results suggested that N259 glycosylation induced by VC was independent of STT3A. On the other hand, downregulation of *Stt3b* significantly impacted N259 glycosylation induced by VC (Fig. 4b). These results indicated that VC-induced N259 glycosylation was STT3B-dependent and, thus, post-translational. If so, N259 glycosylation could be derived from the turnover of the pre-existing N113 glycosylated P4HA1. In MEF cells incubated with VC and CHX, the N113 glycosylated band disappeared, while the top glycosylated band was enhanced (Fig. 4c). Thus, the top glycosylated band was built upon N113 glycosylated P4HA1. Since MAGT1 is in the complex with STT3B as a post-translational modification complex, *Magt1* was silenced to investigate the effect on N259 glycosylation. Downregulation of *Magt1* also significantly reduced N259 glycosylation without affecting P4HA1 protein level (Fig. 4d). These results suggest that N259 is post-translationally modified by STT3B/MAGT1 complex when MEF cells are treated with VC.

Downregulation of *Stt3b* and *Magt1* reduces pepsin-resistant col 1α2 in culture medium by impacting its entry into the Golgi apparatus

The apparent correlation between col 1α2 secretion and appearance of N259 glycosylation on P4HA1 after MEF cells were treated with VC for 6 h suggested a causal relation between N259 glycosylation and proline hydroxylation. In a time-course study, col 1α2 was detected in the medium 3 h after VC treatment. This time point correlated with the appearance of N259 glycans on P4HA1, although limited N259 glycosylation could be detected earlier (Fig. 5a). In addition, pepsin-resistant col 1α2 could be detected when VC concentration was 20 μM or higher, concentrations that also produced increased N259 glycosylation of P4HA1 (Fig. 5b). These results showed a strong correlation between col 1α2 secretion and appearance of N259 glycans on P4HA1.

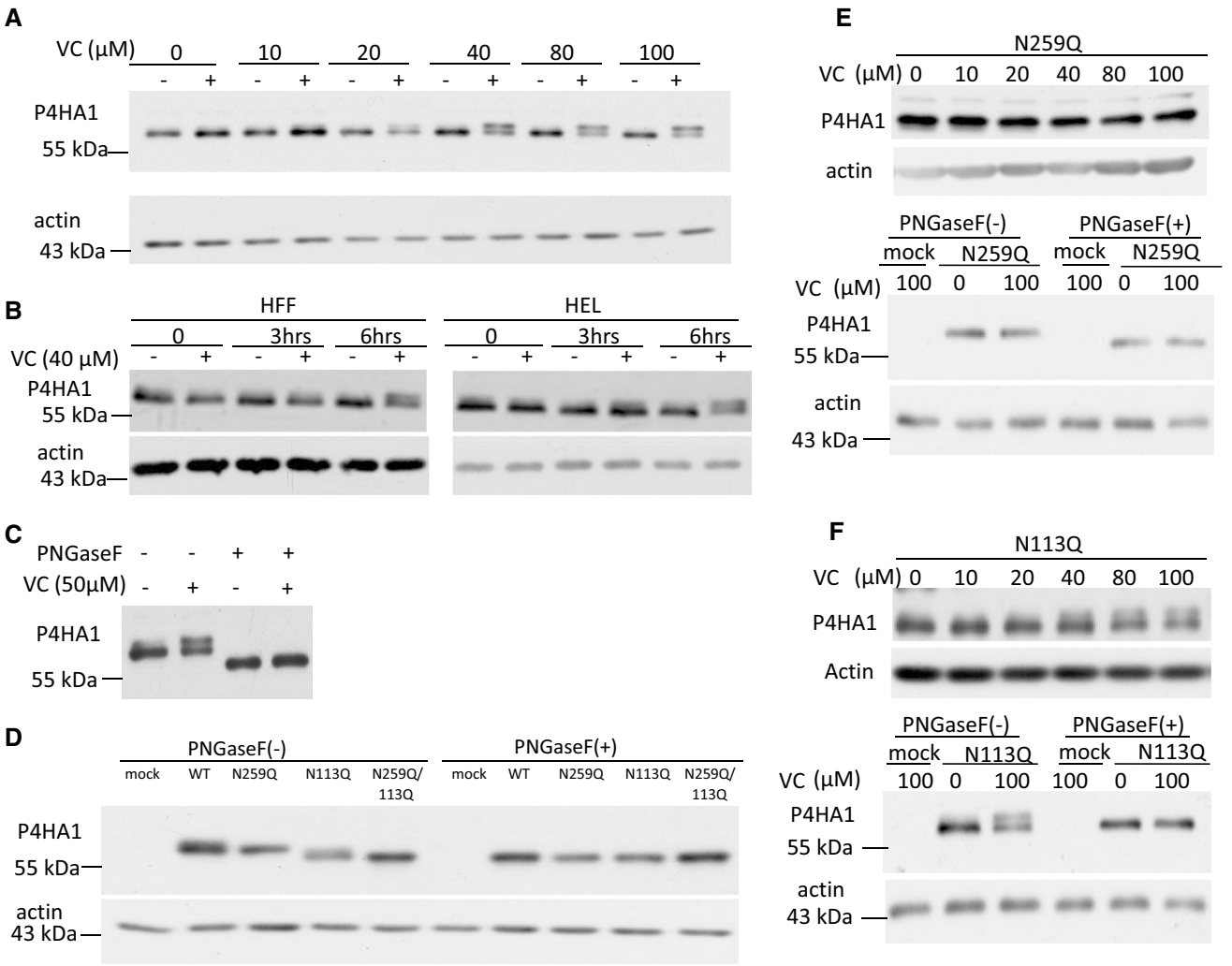

Fig. 3 VC-induced N259-linked glycosylation on P4HA1. **a** Treatment of MEF cells for 6 h with VC concentration of ≥ 40 μM induced expression of an additional protein band reacting to P4HA1 specific antibody. **b** HFF cells and HEL cells also expressed a second protein reacting to antibody specific to P4HA1 at 6 h after VC (40 μM) treatment. **c** PNGaseF treatment of VC-treated and non-treated MEF cell lysate reduced the apparent molecular weight of the proteins reacting to antibody specific for P4HA1. **d** HA-tagged WT, N259Q, N113Q, or N113Q/N259Q double mutants were expressed in *P4ha1*-silenced MEF cells in the absence of VC. The cell lysates were immunoblotted with HA-tag antibody. The N259Q mutant showed the same apparent molecular weight as WT, whereas the apparent molecular weights of N113Q and N113Q/N259Q double mutants were equal but lower than WT (left panel). WT, N113Q, N259Q, and N113Q/N259Q double mutants all showed the same motility as N113Q or N113Q/N259Q double mutants after PNGase F treatment (right panel). **e** N259Q mutated P4HA1 did not show a motility shift after VC treatment (top panel), whereas PNGaseF treatment increased motility of N259Q mutated P4HA1 with or without VC stimulation (third panel). **f** 40 μM or higher concentrations of VC induced an additional protein band reacting to HA-tagged antibody for N113Q-mutated P4HA1 (top panel), which was sensitive to PNGaseF treatment (third panel)

Since STT3B/MAGT1 complex regulated VC-induced N259 glycosylation, *Stt3b* or *Magt1* silencing should impact col 1α2 secretion if N259 glycans play a role for P4HA1 enzymatic activity. When *Stt3b* was downregulated and MEF cells were treated with VC, col 1α2 in the culture medium was slightly reduced and intracellular col 1α2 was increased (Fig. 5c, d). Much of the secreted col 1α2 after *Stt3b* or *Magt1* silencing was not pepsin-resistant (Fig. 5c, d, $n = 4$). Since *Stt3b* or *Magt1* silencing did not reduce P4HA1 protein, *Col 1α2* mRNA, or col 1α2 protein, but did decrease N259 glycosylation of P4HA1 (Fig. 4b, d), these results supported the role of N259 glycosylation in P4HA1 activity and subsequent col 1α2 secretion.

To investigate which step of col 1α2 secretion was affected by decreased N259 glycosylation on P4HA1, intracellular trafficking of col 1α2 was assessed in MEF cells after VC treatment. *Stt3b* or *Magt1* silencing decreased col 1α2 entry into the Golgi apparatus (Fig. 5e, f). In addition, confocal immunofluorescence microscopy showed that most col 1α2 protein was retained in ER when

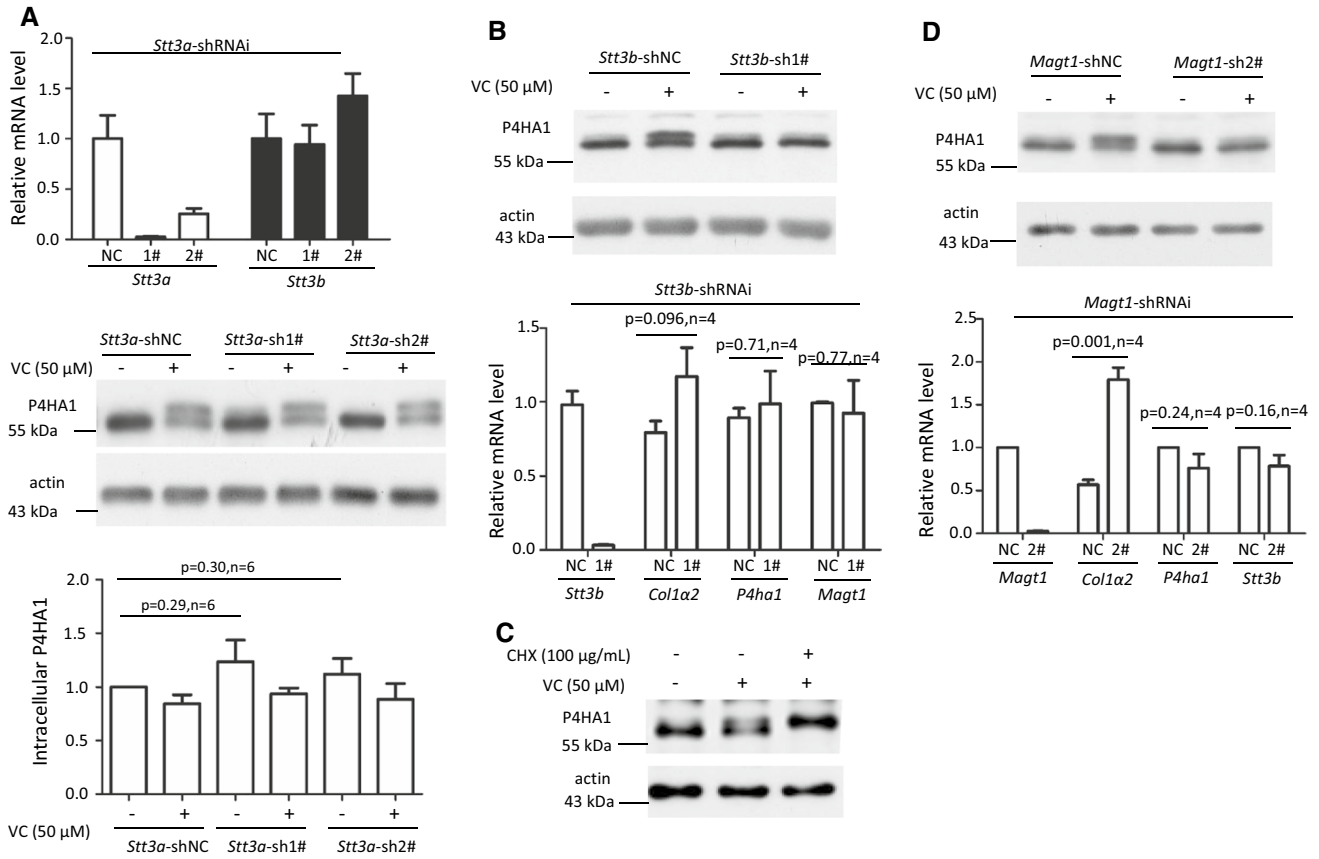

Fig. 4 Silencing *Stt3b* or *Magt1* reduced VC-stimulated N259 glycosylation on P4HA1. **a** Downregulation of *Stt3a* (white bars of top panel) did not reduce N113 glycosylation (middle panel) or the mRNA levels of *Stt3b* (black bars of top panel). NC: *Stt3a*-shRNAi-negative control; 1#: *Stt3a*-shRNAi-1#; 2#: *Stt3a*-shRNAi-2#. Immunoblotting showed that, in the absence or presence of VC, downregulation of *Stt3a* did not affect N113 glycosylation or N259 glycosylation of P4HA1 or P4HA1 protein levels ($n=6$). Silencing of *Stt3b* (**b**) or *Magt1* (**d**) decreased N259 glycosylation on P4HA1 induced by VC without affecting P4HA1 protein levels (left panel). qPCR confirmed efficient downregulation of *Stt3b* (**b**) or *Magt1* (**d**). Silencing *Stt3b* did not affect the mRNA levels of *P4ha1*, *Col1a2*, and *Magt1* (**b**). *NC Stt3b*-shRNAi-negative control; *1# Stt3b*-shRNAi-1# ($n=4$). However, silencing *Magt1* enhanced *Col1a2* but not *P4ha1* and *Stt3b* mRNA levels (**d**). *NC Magt1*-shRNAi-negative control; *2# Magt1*-shRNAi-2# ($n=4$). **c** Incubation of cells with VC plus CHX at the same time for 6 h enhanced N259 glycosylation on P4HA1

Stt3b was downregulated (Supplemental Fig. 5). To verify that silencing *Stt3b* did not alter P4HA1 subcellular localization, leading to reduced proline hydroxylation on Type I collagen, P4HA1 location in the *Stt3b* downregulated cells was assessed. Most P4HA1 co-localized with KDEL-EGFP (Fig. 5g), a protein that indicates ER location. The same phenomenon was observed in the control cells. Thus, silencing *Stt3b* did not alter the subcellular localization of P4HA1. The nuclear staining for P4HA1 was likely to be non-specific, because the staining remained in nuclei in *P4ha1*-silenced cells (Supplemental Fig. 6). These results, together with the observation that silencing *Stt3b* reduced col 1α2 entry into Golgi apparatus, indicated that loss of N259 glycans could alter P4HA1 binding to collagen, thus decreasing collagen hydroxylation and secretion.

Reduced N259 glycosylation on P4HA1 decreased binding between P4HA1 and col 1α2 and attenuated proline hydroxylation on col 1α2

Lack of glycans on P4HA1 was reported to have no effect on its enzymatic activity in vitro [12, 13], but N259 glycans on P4HA1 affected col 1α2 secretion in MEF cells. Therefore, the effect of N259 glycosylation on the interactions between P4HA1 and col 1α2 in cells was assessed. Co-immunoprecipitation (Co-IP) of P4HA1 and col 1α2 with anti-P4HA1 or anti-Type I collagen antibody showed significantly less P4HA1 which was associated with col 1α2 in *Stt3b*-silenced cells (Fig. 6a, b, $n=3$). The decreased association could impact on subsequent hydroxylation of the substrate (col 1α2).

To prove that P4HA1 without N259 glycosylation hydroxylated fewer proline residues on col 1α2, col 1α2 from *Stt3b*-silenced and control MEF cells was assessed by mass spectrometry. Although similar amounts of col 1α2 were concentrated from *Stt3b*-silenced and control MEF cells (Fig. 6c), significant differences in proline hydroxylation on col 1α2 were noted. When *Stt3b* was silenced, col 1α2 had reduced proline hydroxylation, especially on proline at sites 96, 294, 777, 795, and 1038 (based on numbering from the N-terminus of the immature protein) (Fig. 6d). However, the reduction of proline hydroxylation was not universal; significantly more hydroxylated proline was detected at sites 564 and 921 on col 1α2 (Fig. 6d). Similar results were observed for col 1α1 with reduced proline hydroxylation detected at eight sites and more hydroxylated proline found at four sites (Supplemental Fig. 7). Three sets of mass spectrometry results showed similar findings (Supplemental Table 1). These data supported the idea that VC-induced N-linked glycosylation of P4HA1 alters the association between enzyme and substrate and the subsequent proline hydroxylation and collagen maturation.

Discussion

Type I collagen is the most abundant collagen in the body and collagen production is essential for many physiological processes including tissue repair. Understanding how collagen matures and is secreted will aid in understanding disease conditions due to deficiency or over-deposition of collagen. VC is a co-factor for collagen homeostasis in haplorrhini (including humans, guinea pigs, and some bats), which lack L-gulonolactone oxidase. Although the chemical reactions have been largely solved for proline and lysine hydroxylation on collagen [20–24], it remains unclear how specific proline and lysine sites on collagen are selected by these hydroxylases. Our studies show that prolyl hydroxylation is modulated by VC-induced enhancement of N259 glycosylation on P4HA1 (Fig. 6). However, N259 glycosylation does not seem to enhance affinity between P4HA1 and Type I collagen, because no enrichment of N259 glycosylated P4HA1 was detected in the Co-IP studies (Fig. 6b). The mechanism by which this occurs warrants further investigation.

Mammalian cells possess two oligosaccharyltransferase complexes (STT3A and STT3B) to catalyze N-linked glycosylation, which may facilitate protein folding, enhance protein stability, modify immune recognition, and regulate protein interactions [25, 26]. Glycosylation of many NXT/S sites in glycoproteins is not reduced when *Stt3a* or *Stt3b* is silenced by siRNA-based method [27, 28]. Downregulation of *Stt3a* or *Stt3b* does not affect N113 glycosylation on P4HA1. This could be due to low efficiency of downregulation or to the existence of other oligosaccharyltransferase complexes. Work is in progress to understand this. In addition, the effect of N113 glycosylation on P4HA1 activity and collagen maturation remains unclear.

Fig. 5 VC-induced N259-linked glycosylation on P4HA1 altered col 1α2 secretion. Enhanced col 1α2 in the culture medium and pepsin-resistant col 1α2 could be detected 3 h after VC treatment of MEF cells (top two panels) (**a**) or when VC concentration was ≥ 40 μM (top two panels) (**b**). MEF cells were treated with 50 μM of VC for different times (**a**) or with different concentrations of VC for 6 h (**b**). Col 1α2 in cell lysates or in the culture medium was detected. Quantification of collagen in the medium and N113/N259 and N113 glycosylated P4HA1 confirmed a correlation between N259 glycosylation and collagen in the medium (**a**, **b** graphic pictures, $n = 3$). N113/N259 glycosylated P4HA1 (or di-glycosylated P4HA1, Di-) is the top band; N113 glycosylated P4HA1 (or mono-glycosylated P4HA1, Mono-) is the bottom band. Silencing *Stt3b* (**c**, **e**, **g**) or *Magt1* (**d**, **f**) reduced VC-induced pepsin-resistant col 1α2 in the culture medium (**c**, **d**) and VC-activated col 1α2 (red) entry into Golgi apparatus (green, indicated by arrow) (**e**, **f**). However, silencing *Stt3b* did not alter P4HA1 localization in ER (**g**). *Stt3b*- or *Magt1*-silenced or control MEF cells were treated with 50 μM of VC or without VC treatment for 6 h, col 1α2 was detected in the cell lysates or in the culture medium (**c**, **d**) or was detected by confocal immunofluorescence staining (**e**–**g**). The ER marker KDEL-EGFP was expressed in *Stt3b* downregulated MEF cells. P4HA1 was labeled with polyclonal antibody specific to P4HA1. Most P4HA1 co-localized with KDEL-EGFP. Nuclear staining for P4HA1 was non-specific. Quantification of intracellular collagen and pepsin-resistant collagen showed that silencing *Stt3b* or *Magt1* significantly altered VC-induced pepsin-resistant collagen ($n = 4$). Laminin was used as a loading control for culture medium protein, whereas actin was used as a loading control for cell lysate. *NT* no VC treatment, *VC* VC treatment. Asterisk indicates col 1α2. Densitometry of immunoblots was quantified using Image J and depicted graphically

Downregulation of *Stt3b* or *Magt1* does not eliminate VC-stimulated secretion of pepsin-resistant col 1α2 into the culture medium (Fig. 5c, d). Thus, there is an additional mechanism for VC-activated Type I collagen secretion. Interestingly, it has been reported that VC can stimulate procollagen biosynthesis by enhancing the association between endoplasmic reticulum and ribosome [29]. Whether this is the mechanism responsible for the observed col 1α2 in the culture medium of *Stt3b*- or *Magt1*-silenced cells after incubation with VC remains to be investigated.

When *Magt1* is silenced, the level of *Col1a2* mRNA is significantly elevated (Fig. 4d, right panel), without a concomitant increase in intracellular protein level of col 1α2 (Fig. 5d). The explanation for this remains unclear. *Col1a2* translation efficacy or protein stability could be reduced.

It is reported that glycans on P4HA1 do not change its total enzymatic activity when purified enzymes are used to test enzymatic activity in vitro [12, 13]. In *Stt3b*-silenced cells, reduced N259 glycosylation decreases P4HA1 association with col 1α2 and altered hydroxylation of specific proline residues. The mechanism by which P4HA1 N259 glycosylation alters P4HA1 association with col 1α2 or

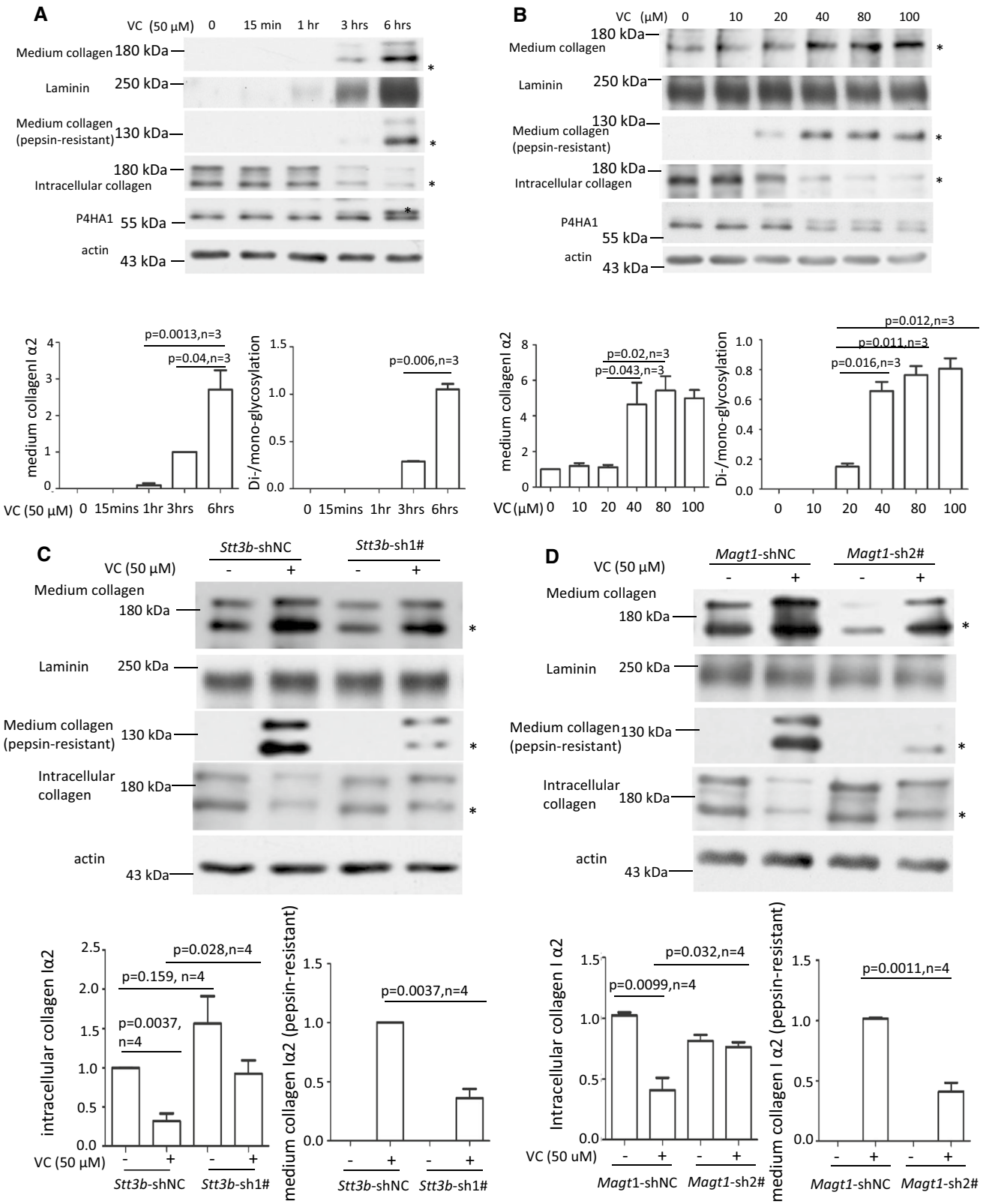
A
VC (50 μM) 0 15 min 1 hr 3 hrs 6 hrs
Medium collagen 180 kDa
Laminin 250 kDa
Medium collagen (pepsin-resistant) 130 kDa
180 kDa
Intracellular collagen
P4HA1 55 kDa
actin 43 kDa
B
VC (μM) 0 10 20 40 80 100
Medium collagen 180 kDa
Laminin 250 kDa
Medium collagen (pepsin-resistant) 130 kDa
180 kDa
Intracellular collagen
P4HA1 55 kDa
actin 43 kDa
medium collagenI α2
p=0.0013,n=3
p=0.04,n=3
Di-/mono-glycosylation
p=0.006,n=3
VC (50 μM) 0 15mins 1hr 3hrs 6hrs
medium collagenI α2
p=0.02,n=3
p=0.043,n=3
Di-/mono-glycosylation
p=0.012,n=3
p=0.011,n=3
p=0.016,n=3
VC (μM) 0 10 20 40 80 100
C
Stt3b-shNC
Stt3b-sh1#
VC (50 μM) - + - +
Medium collagen 180 kDa
Laminin 250 kDa
Medium collagen (pepsin-resistant) 130 kDa
Intracellular collagen 180 kDa
actin 43 kDa
intracellular collagen Iα2
p=0.028,n=4
p=0.159, n=4
p=0.0037, n=4
VC (50 μM) - + - +
Stt3b-shNC Stt3b-sh1#
medium collagen Iα2 (pepsin-resistant)
p=0.0037,n=4
Stt3b-shNC Stt3b-sh1#
D
Magt1-shNC
Magt1-sh2#
VC (50 μM) - + - +
Medium collagen 180 kDa
Laminin 250 kDa
Medium collagen (pepsin-resistant) 130 kDa
Intracellular collagen 180 kDa
actin 43 kDa
Intracellular collagen I α2
p=0.032,n=4
p=0.0099,n=4
VC (50 uM) - + - +
Magt1-shNC Magt1-sh2#
medium collagen I α2 (pepsin-resistant)
p=0.0011,n=4
Magt1-shNC Magt1-sh2#

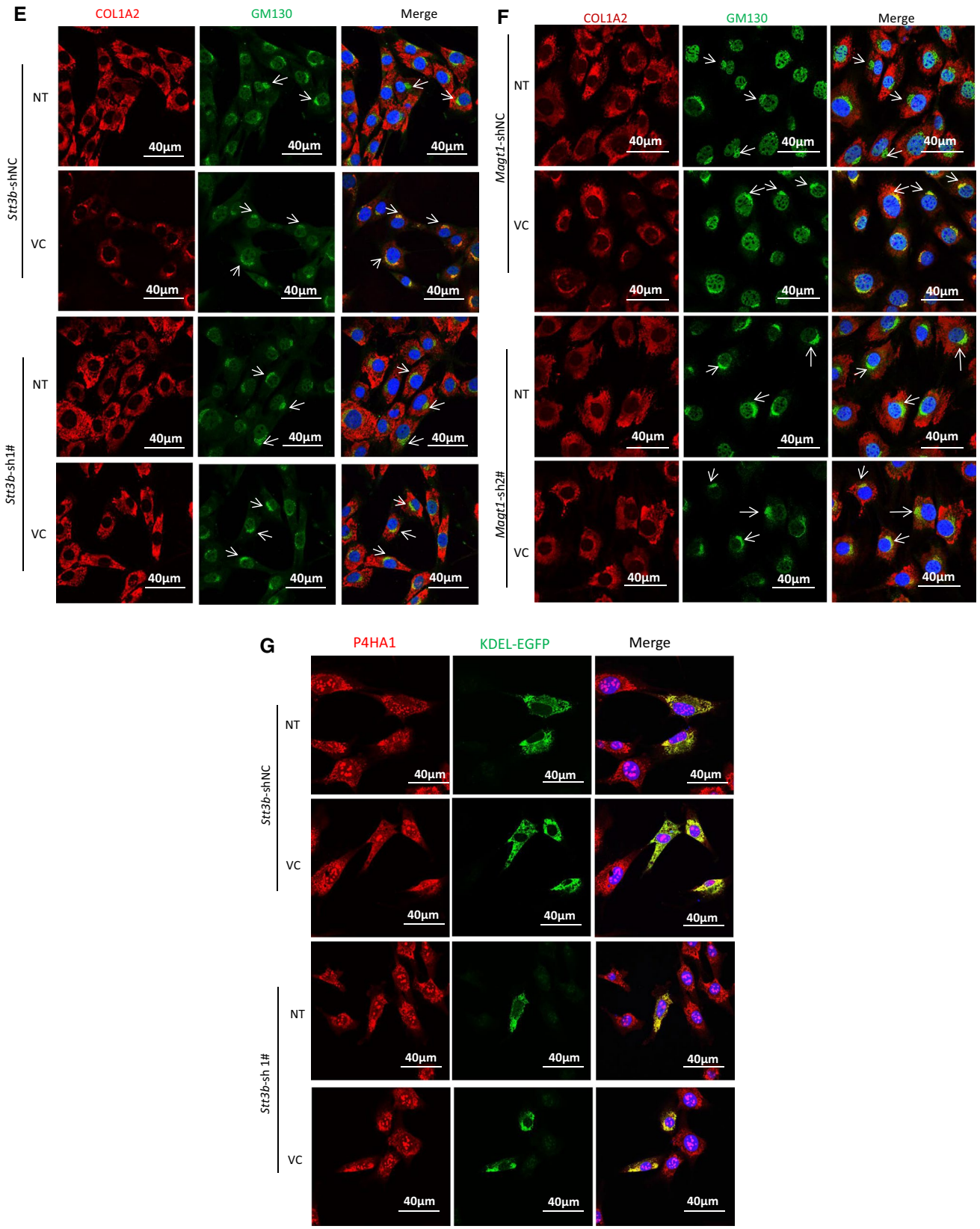

Fig. 5 (continued)

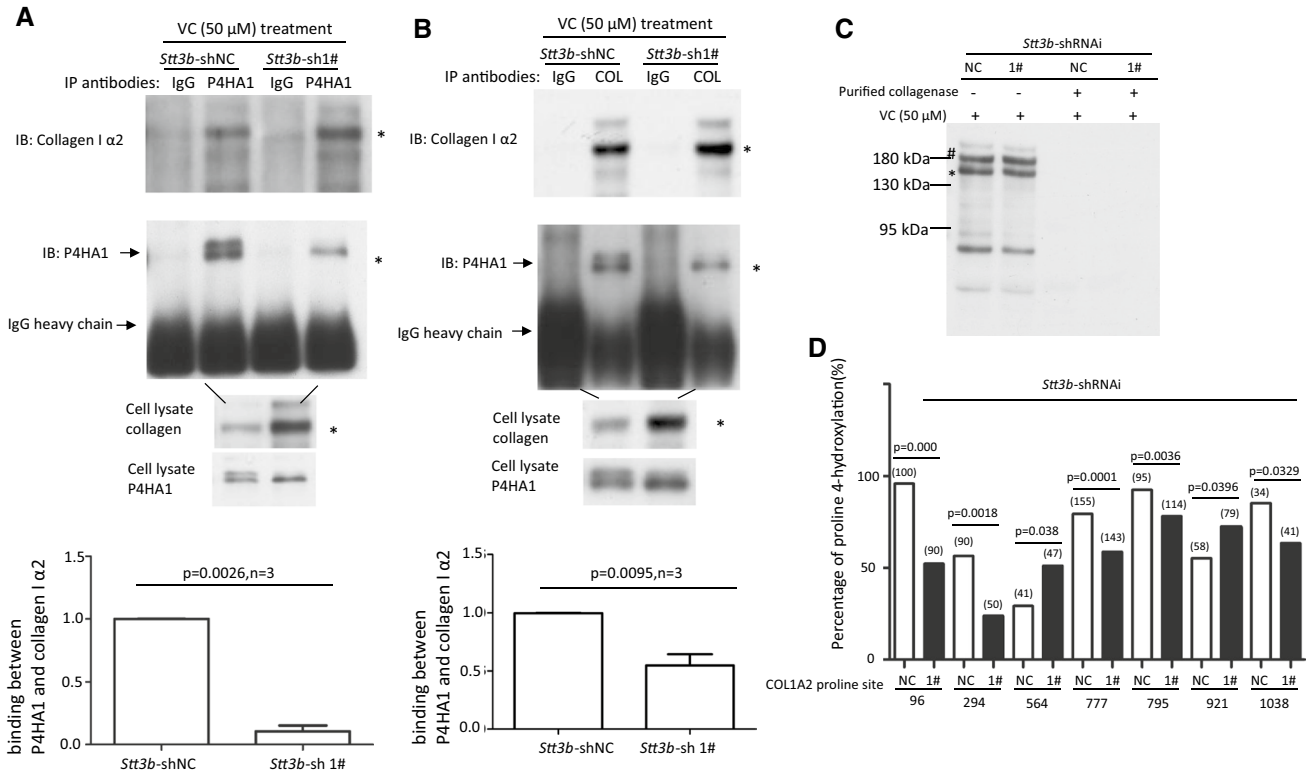

Fig. 6 Lack of N259 glycosylation on P4HA1 reduces P4HA1 association with col 1α2. Co-IP was performed with anti-P4HA1 (**a**) or anti-Type I collagen (**b**) antibody (2 μg) using 1 mL of cell lysate. Co-purified col 1α2 and P4HA1 were identified by immunoblot analysis using corresponding antibodies. IgG heavy chain was marked. Immunoblot analysis for col 1α2 was performed with 20 μL of cell lysate. The presence of N259 glycosylation on P4HA1 was indicated by two bands recognized by P4HA1 antibody. Statistical analysis showed that the presence of N259 glycans on P4HA1 significantly enhanced the association between col 1α2 and P4HA1 when Co-IP was performed with anti-P4HA1 antibody ($n=3$) (**a**) and anti-Type I collagen antibody ($n=3$) (**b**). The ratio between P4HA1 and col 1α2 in control MEF cells was defined as 1. The relative ratio between P4HA1 and col 1α2 in *Stt3b*-silenced cells was calculated based on densitometry on immunoblots assessed by Image J using ratio between P4HA1 and col 1α2 from control cells as standard. **c** Immunoblotting with Type I collagen antibody confirmed that Type I collagen was loaded equivalently from *Stt3b*-silenced or control MEF cells (indicated by asterisk and hash). The slices in a Coomassie brilliant blue stained gel corresponding to the immunoblotting were cut and subjected to mass spectrometry analysis. **d** Significant differences in proline hydroxylation on col 1α2 were observed between *Stt3b*-silenced and control cells. The number of peptide containing specific proline sites identified by mass spectrometry was included in the bracket. *p* value was indicated for each proline site which showed significant differences in hydroxylation between control and *Stt3b*-silenced cells. *NC Stt3b*-shRNAi-negative control (white bars); *1# Stt3b*-shRNAi-1# (black bars). Chi-square analysis was used to analyze differences at each proline site on Type I collagen

selection of proline residues for hydroxylation remains unknown. Silencing *Stt3b* and subsequent decrease in N259 glycosylation of P4HA1 appear to reduce P4HA1 binding to its antibody when the antibody was used in Co-IP studies (Fig. 6a).

Although N259 glycosylation on P4HA1 modulates proline hydroxylation, it does not have a universal effect on col 1α2. In *Stt3b*-silenced cells, five proline sites of col 1α2 had decreased hydroxylation and two had increased hydroxylation (Fig. 6). This suggests that N259 glycans fine tune the interaction between col 1α2 and P4HA1. Similar effects were detected for col 1α1. Identification of the mechanism by which the N259 glycans regulate proline hydroxylation at specific sites of collagen will require detailed structural studies.

Materials and methods

Antibodies and reagents

Ascorbic acid (A7506) and ethyl-3,4-dihydroxybenzoate (EDHB) (E24859) were purchased from Sigma-Aldrich (Darmstadt, Germany). GM130 rabbit polyclonal antibody (A5344), P4HA1 rabbit polyclonal antibody (A3999), Rabbit polyclonal antibody anti-Laminin (LAMC1) (A16020), Rabbit anti-HA-Tag polyclonal antibody (AE036), HRP-conjugated goat anti-mouse IgG (AS003), goat anti-rabbit IgG (AS014), and HRP-conjugated rabbit anti-goat IgG (AS029) were purchased from ABclonal (Cambridge, MA, USA). Goat anti-human Type I collagen (1310-01s) antibody, which was shown to react to mouse Type I collagen,

was purchased from Southern Biotech (Birmingham, AL, USA). Proteinase inhibitor cocktail (11697498001) and 4′, 6-diamidino-2-phenylindole (DAPI) (10236276001) were purchased from Roche Diagnostics (Mannheim, Germany). Alexa Fluor 555 conjugated donkey anti-goat IgG (ANT082) was purchased from AntGene Biotech (Wuhan, China). Alexa Fluor 488 conjugated donkey anti-rabbit IgG (A21206) was purchased from Invitrogen (Eugene, OR, USA). Protein G Agarose Fast Flow beads (16-266) were purchased from Merck Millipore (Darmstadt, Germany). PNGase F (P0704S) was purchased from New England BioLabs (Beverly, MA, USA).

Fibroblast cell culture

MEF cells were purchased from ATCC and were grown in Dulbecco's modified Eagle's medium (DMEM; high glucose without ascorbic acid), supplemented with 1% antibiotic Penicillin–Streptomycin solution (PS) (03-031-1, Biological Industries, Kibbutz Beit-Haemek, Israel) plus 10% fetal bovine serum (FBS) (04-001-1, Biological Industries, Kibbutz Beit-Haemek, Israel). HFF cells and HEL cells were isolated and provided by Dr. Min-hua Luo at Wuhan Institute of Virology, Chinese Academy of Sciences, and used between cell passages six and ten. All cells were cultured in a 37 °C, 5% CO_2, 95% humidity incubator.

To evaluate the effect of VC on collagen production, all fibroblasts were seeded in 6-well plates and cultured for 24 h in 10% FBS DMEM until reaching 85% confluence. Cells were then maintained in 1% FBS DMEM overnight and stimulated for 0, 1, 3, and 6 h in serum-free DMEM containing 50 μM VC or as indicated in the manuscript. At the end of treatment, conditioned media were collected and spun at 1000×*g* for 30 min (minutes). Collected media containing Type I collagen were precipitated with 176 mg/mL ammonium sulfate for 24 h at 4 °C. Samples were then centrifuged at 10,000×*g* for 1 h, and the pellet was solubilized in a solution containing 0.4 M NaCl, 0.1 M Tris, and pH 7.4.

The cells were rinsed twice with ice-cold phosphate-buffered saline (PBS) and scraped into cell lysis buffer (20 mM Tris–HCl (pH 7.5), 150 mM NaCl, 1 mM EDTA, 1 mM EGTA, 2.5 mM sodium pyrophosphate, 1 mM b-glycerophosphate, 1 mM Na_3VO_4, 1% Triton, 1 mM PMSF, and 1× proteinase inhibitor cocktail) and sonicated at 1 J for 6 s on ice. The cell debris was removed by centrifugation and protein concentration was quantified using a Bio-Rad Protein Assay Kit II.

SDS-PAGE and Western blotting analysis

To determine the level of type I collagen secreted from control and VC-treated fibroblasts, western blots were performed on the cell lysate and conditioned media prepared as above. The samples were mixed with 4× sodium dodecyl sulfate (SDS) reducing sample buffer [40% glycerol (V/V), 250 mM Tris–HCl pH 6.8 (V/V), 8% sodium dodecyl sulfate (W/V), 0.04% bromophenol blue (W/V), and 20% 2-mercaptoethanol (ME) (V/V)]. The samples were then heated at 100 °C for 10 min and loaded in a 7.5% SDS-PAGE. After electrophoresis, proteins were transferred to nitrocellulose membranes (HATF00010, Merck Millipore), which were further blocked with bovine serum albumin (BSA) in tris-buffered saline (TBS) with 0.1% Tween-20 (TBST) at room temperature (RT) for 3 h and then incubated with anti-Type I collagen antibody (0.4 μg/mL), anti-Laminin antibody (1 μg/mL), anti-P4HA1 (1 μg/mL), anti-P4HA2 (1 μg/mL), or anti-actin antibody (0.2 μg/mL) overnight at 4 °C. Bound primary antibodies were detected with rabbit anti-goat, goat anti-rabbit or mouse HRP-conjugated secondary antibody (0.12 μg/mL), respectively. The amount of type I collagen was quantified by densitometry using the Image J software (NIH) and were normalized to actin loading controls. The data were presented as the mean ± SEM.

Intracellular and medium collagen stability in *P4ha1* silencing MEF cells

To determine intracellular collagen stability after *P4ha1* silencing, *P4ha1*-silenced or control MEF cells were incubated with 100 μg/mL of CHX, the protein translation inhibitor, for various times. Cell lysates were collected and assayed by immunoblot analysis as indicated.

To determine medium collagen stability after *P4ha1* silencing, *P4ha1*-silenced or control MEF cells were treated with 50 μM VC for 3 h, and then 100 μg/mL of CHX was added for varying times (time 0 was defined as time of CHX addition). After treatment, cell lysates and media were collected and assayed by immunoblot analysis as indicated.

Immunofluorescence (IF) staining

To investigate the effect of silencing *Stt3b* or *Magt1* on Type I collagen's entry into Golgi apparatus after VC treatment, cells were seeded on confocal petri dishes (801002, NEST, China) and cultured for 24 h in 10% FBS DMEM until reaching 85% confluence. Cells were then maintained in DMEM containing 1% FBS overnight and stimulated for 6 h in DMEM containing 1% FBS with 50 μM VC. After treatment, IF staining was performed to detect the col 1α2 localization. The cells were rinsed twice with ice-cold PBS and then fixed with 4% (W/V) paraformaldehyde in PBS for 10 min at RT. After washing three times, fixed cells were permeabilized with 0.1% (V/V) Triton X-100 in PBST for 10 min. Permeabilized cells were blocked with 5% BSA in PBST for 2 h at RT. To detect the co-localization of col1α2

Table 1 The *P4ha1*, *P4ha2*, *Stt3a*, *Stt3b,* and *Magt1* sequences targeted by shRNAi or sgRNA

Name sequence
P4ha1-shRNAi-sh3# 5′-GGAGTGCAACATAAGTCTTTC-3′
P4ha1-shRNAi-sh4# 5′-GCTGTCTACTGTAGATAAAGT-3′
Stt3b-shRNAi-sh1# 5′-GCTGCTTGCTTCATTGCTATC -3′
Magt1-shRNAi-sh2# 5′-GGACTTGTGTATCTGCGAAGA-3′
Stt3a-shRNAi-sh1# 5′-GCATGCTGCTTACTTACTACA-3′
Stt3a-shRNAi-sh2# 5′-GCTGTAATGGTGCGTCTAATG-3′
P4ha2-sgRNA-1# 5′-CGATCTGATTTACGCAGAGA-3′
P4ha2-sgRNA-4# 5′-AGATCAGCTGCCGACCCCGA-3′

and Golgi apparatus, goat anti-type I collagen or rabbit anti-GM130 antibody were applied for 2 h at RT. Bound primary antibodies were then detected with Alexa Fluor-conjugated donkey anti-rabbit or goat IgG. Nuclei were counterstained with DAPI (500 ng/mL) for 5 min.

To investigate whether silencing *Stt3b* affects P4HA1 subcellular localization, *Stt3b*-silenced and control MEF cells were seeded on confocal petri dishes and cultured for 12 h in 10% FBS DMEM until 50% confluent. The ER marker EGFP-KDEL was transiently transfected in above cells with Lipofectamine 2000 reagent according to the manufacturer's protocol. Briefly, the Lipofectamine 2000 reagent (6 μL) or vector (2 μg) was diluted in Opti-MEM Medium (150 μL). The diluted vector was added to diluted Lipofectamine 2000 Reagent (1:1 ratio). After 20 min incubation, the mixture was added to the cells, and they were cultured for 24 h. Then, cells were maintained in DMEM containing 1% FBS overnight and stimulated for 6 h in DMEM containing 1% FBS, 50 μM VC. IF staining was performed as above.

Establishment of stable knockdown and knockout cell lines

To generate stable *P4ha1*, *Stt3a*, *Stt3b* and *Magt1*-silenced cells, shRNA against *P4ha1*, *Stt3a*, *Stt3b*, and *Magt1* were designed using online BLOCK-iT™ RNAi Designer software.

shRNAi against the above genes were subcloned into pLKO.1 Vector (VEC-PRT-0002,Oligoengine, US) according to the manufacturer's instructions. Briefly, the oligonucleotide sequences were annealed and ligated into pLKO.1 Vector at 22 °C for 2 h. The ligation product was transformed into *E. coli* (DH5a). Positive clones were selected after *EcoRI* and *NcoI* digestion showing two fragments, a 2 kb fragment and a 5 kb fragment.

Lentivirus particles were generated. Briefly, HEK293T cells were co-transfected with pLKO.1 recombinant construct and the packaging plasmids pMD2.G and psPAX2 (a gift supplied by Professor Cunyi Zheng, Wuhan University, China) for 72 h. Media were then collected and filtered with a 0.45 μm filter. The shRNA retroviral stocks were used to infect MEF cells in the presence of 7.5 μg/mL Polybrene (107689, Sigma, USA). The stably silenced cells were screened with 2 μg/ml puromycin (ant-pr-1, InvivoGen, USA) for at least 2 weeks. The interference effect was assessed with qPCR and immunoblotting. The target sequences by shRNAi are listed in Table 1.

To generate *P4ha2* null MEF cells, CRISPR/Cas systems were used. The primers for *P4ha2* knockout in MEF cells are listed in Table 1. To knockout *P4ha2* in MEF cells, the primers (100 μM) were annealed and ligated to pX459. The recombinant plasmids were sequenced and transfected into MEF cells with Lipofectamine 2000 reagent according to the manufacturer's protocol. Three day post-transfection, cells were screened with 2 μg/mL puromycin. *P4ha2* knockout MEF cells were verified by DNA sequencing and western blotting.

RNA isolation and quantitative real-time PCR (qPCR)

To evaluate whether silencing *P4ha1, Stt3b, Magt1,* or *Stt3a* in MEF cells influenced other genes expression, RNA was isolated from control and corresponding silenced cells using the total RNA purification kit (GeneMark, number TR01-150, Taichung, Taiwan). RNA (1 μg) was reverse transcribed using a PrimeScript TM RT reagent kit (TaKaRa, number RR047A, Shiga, Japan). qPCR was carried out using SYBR Green Supermix (Bio-Rad, number 170-8882AP, Hercules, CA, USA) on a Bio-Rad Connect TM real-time PCR instrument (CFX Connect TM Optics Module). Each reaction volume of 10 μL contained cDNA templates, primer pairs, and SYBR Green Supermix. Amplification occurred after initial denaturation at 95 °C for 3 min, followed by 40 cycles at 95 °C for 10 s, 53 °C for 15 s, and 72 °C for 15 s. *β-Actin* was used as a reference gene. Gene-specific primers are listed in Table 2.

Construction of plasmids

pHAGE-P4HA1 was constructed as below. Briefly, P4HA1 was amplified with primers listed in Table 3 using the cDNA from MEF cells. The PCR amplified fragment was gel purified and digested with *NotI* and *NheI* at 37 °C for 2 h. The digested sample was further gel purified and ligated into pHAGE-CMV-MCS-IZsGreen vector by standard molecular biology techniques.

Constructs of pHAGE-HA-tagged-P4HA1 were amplified through insertion mutation with mutagenic primers listed in Table 3. Briefly, pHAGE-P4HA1 was amplified with mutagenic primers containing influenza hemagglutinin epitope (HA) sequence. The amplified sample was digested with *DpnI* at 37 °C for 2 h. The digested sample was directly transformed into *E. coli* (DH5a). pHAGE-HA-tagged-P4HA1-N113Q, P4HA1-N259Q, and P4HA1-N113Q/

Table 2 Primers used to amplify *Col1α2*, *β-Actin, P4ha1, Stt3b, Magt1,* and *Stt3a* from MEF cells

Gene name sequence
Col1α2
Sense: 5′-GCGGTGAAGAAGGAAAGAGA-3′
Antisense: 5′- CCAGGAGACCCAGGAAGAC-3′
P4ha1
Sense: 5′-CAAGCAGGAGGACGAGTGG-3′
Antisense: 5′-TGGGTTTGAAATGGTGGC-3′
P4ha2
Sense: 5′- GTGTGGACGACTGCTTTGG-3′
Antisense: 5′-TTGACAGTGATTTCCCTCTTTCT-3′
Stt3b
Sense: 5′-TGGTCCTTGCCTCCTACAAT-3′
Antisense: 5′-GCCAATCACTCCTCCGAAA-3′
Magt1
Sense: 5′-TGTTATTGGTGGACTTGTGTATC-3′
Antisense: 5′-GAAGAACGATGTGGGTTTCA-3′
Stt3a
Sense: 5′-CCTGTCTGATGCTCGGATTT-3′
Antisense: 5′-CCCACTCGCCACCTCATT-3′
β-Actin
Sense: 5′-CGTGCGTGACATCAAAGAGAAGC-3′
Antisense: 5′-TGGATGCCACAGGATTCCATACC-3′

N259Q (double mutations) were mutated with the corresponding primers listed in Table 3.

The lentiviral packaging system consisted of one expression plasmid: pHAGE-CMV-MCS-IZsGreen and two packaging plasmids: pMD2.G and psPAX2. Generation of lentivirus particles containing WT and mutant P4HA1 was similar to shRNA retrovirus described above. The lentivirus stocks were used to infect *P4ha1*-silenced MEF cells.

Constructions of pcDNA3.1-EGFP-KDEL were amplified through overlap PCR with the corresponding primers listed in Table 3. The EGFP containing the amino acids KDEL was amplified from the pEGFP-N1 vector (the reverse primer containing the nucleotide sequence of KDEL motif). Signal peptide of calreticulin was amplified using the cDNA from MEF cells. These two DNA fragments were then mixed and annealed to obtain hybrid duplexes. The resulting hybrids were then extended and amplified to yield recombinant PCR products. The product was digested with *NotI* and *XbaI* and ligated into pcDNA3.1.

Glycosidase assay

PNGase F treatment was performed according to the manufacturer's instructions. Briefly, MEF cells were stimulated with 50 μM VC for 6 h. Cell lysates were extracted and incubated with glycoprotein denaturing buffer. The samples were boiled for 10 min and then treated with PNGase F for 1 h at 37 °C. PNGase F treated samples were then assayed by immunoblotting as above.

N113/N259 glycosylated P4HA1 and N113 glycosylated P4HA1 bands were quantitated by densitometry using Image J. Densitometry of collagen bands and glycosylated P4HA1 bands were depicted graphically.

To investigate which glycosylation site was VC treatment dependent, stably transfected HA-tagged N113Q and N259Q P4HA1 cells were stimulated with 100 μM VC for 6 h. The cell lysates were treated with PNGase F as above and used for immunoblot analysis to assess glycosylation status of N113Q and N259Q mutated P4HA1.

To investigate if the STT3B/MAGT1 complex glycosylated newly made P4HA1 or pre-existing N113-glycan form of P4HA1, MEF cells were maintained in DMEM containing 1% FBS overnight and treated for 6 h in

Table 3 Primers used to amplify *P4ha1* and EGFP-KDEL and mutate *P4ha1*

Gene name sequence
*P4ha*1
Sense: 5′ATTTGCGGCCGCCACCATGATCTGGGTTGTTTTAATGA-3′
Antisense: 5′-CTAGCTAGCTTCCAATTCTGACAGGGTG-3′
HA-tagged-*P4ha1*
Sense: 5′-CGTAAAAAACCCTGGATGAGCGTAATCTGGAACATCGTATGGGT AGGCTAAAGACTGAGGAAG-3′
Antisense: 5′-CTTCCTCAGTCTTTAGCCTACCCATACGATGTTCCAGATTACGCT CATCCAGGGTTTTTTACG-3′
P4ha1-N113Q
Sense: 5′-ACTGCCTCTGAATGGTTAGTTGAGAGATGAAGCCATCCGAC-3′
Antisense: 5′-GTCGGATGGCTTCATCTCTCAACTAACCATTCAGAGGCAGT-3′
P4ha1-N259Q
Sense: 5′-GGTCGCCCGACGCTGACTTTTGGGCATCTTTTTCTTTACTCA-3′
Antisense: 5′-TGAGTAAAGAAAAAGATGCCCAAAAGTCAGCGTCGGGCGACC-3′
Signal peptide of Calreticulin
Sense: 5′-ATTTGCGGCCGCCACCATGCTCCTTTCGGTGCCG-3′
Antisense: 5′-CAGCTCCTCGCCCTTGCTCACTGCGGCGGCCAGGCCGAGGA-3′
Egfp
Sense: 5′-TCCTCGGCCTGGCCGCCGCAGTGAGCAAGGGCGAGGAGCTG-3′
Antisense: 5′-GCTCTAGATTACAGCTCATCCTTGTACAGCTCGTCCATGCC-3′

serum-free DMEM containing 50 μM VC alone, or 50 μM VC plus 100 μg/mL CHX. After treatment, cell lysates were immunoblotted to visualize the glycosylation status of P4HA1.

Co-IP

To detect the interaction between P4HA1 and col 1α2 in silenced or control MEF cells, *Stt3b*-silenced or control cells were grown in 10% FBS DMEM until reaching 85% confluence. The cells were then maintained in DMEM containing 1% FBS overnight and treated for 6 h in serum-free DMEM containing 50 μM VC. Cell lysates were collected as above. Co-IP was performed with 2 μg of anti-P4HA1 antibody or anti-Type I collagen antibody and their corresponding isotype control antibodies. Briefly, 1 mL of cell lysate was incubated with P4HA1 or Type I collagen antibody and 40 μL of 50% slurry of protein G Sepharose beads (16-266, Merck Millipore) at 4 °C overnight. After washing six times with cell lysis buffer, the beads were boiled in 40 μL 2× SDS reducing sample buffer. 20 μL cell lysates were used for Co-IP and proteins were separated on a 7.5% SDS-PAGE.

Liquid chromatograph–mass spectrometer (LC–MS)

To enrich media Type I collagen for LC–MS analysis, eight 15 cm Petri dishes of *Stt3b*-silenced and twelve 15 cm Petri dishes of control cells were treated with VC as above. Conditioned media were collected and spun at 1000×*g* for 30 min. Media containing Type I collagen were concentrated with Amicon Ultra-15, 30 K (UFC 903001, Millipore). The concentrated media were mixed with 4× SDS reducing sample buffer and separated on a 7.5% SDS-PAGE. The gel was stained by Coomassie brilliant blue. The slices corresponding to immunoblot containing Type I collagen were cut off for LC–MS. The peptide solutions were digested with trypsin and analyzed by Orbitrap Elite LC–MS/MS (Thermo, USA). Peptides were separated on the C18 Reversed Phase HPLC Columns (1.8 μm, 0.15 × 1.00 mm) at a flow rate of 600 nL/min with a binary gradient. Identification of peptides containing Pro residues and their hydroxylated forms was performed by searching the acquired MS/MS spectra against the Uniprot-Mus musculus.fasta using Proteome Discoverer 1.4 software (Thermo). Quantitation of Pro 4-hydroxylation (4-Hyp) at a specific Pro site was calculated using the ratio of the number of peptides containing corresponding specific 4-Hyp site to the number of total peptides containing corresponding 4-Hyp and Pro site. The experiments were repeated three times.

Statistical analyses

Two major statistical tests were applied in this manuscript. When comparing the measurements under two treatment groups, a two-sample *t* test was performed to determine if the two measurements were significantly different. When comparing the proportions of two groups, a Chi-squared test was performed to determine if the two proportions were significantly different. All the experiments were repeated at least three times and analyzed by two-tailed *t* test. Densitometry of immunoblots was quantified by Image J. Chi-square test was used to assess the hydroxylated proline data obtained from Mass Spectrometry. Quantitative data were expressed as the mean ± standard error of the mean. $p < 0.05$ was considered statistically significant.

Acknowledgements We thank the Core Facility and Technical Support, Wuhan Institute of Virology for assistance with confocal microscope (Dr. Ding Gao) and flow cytometry (Ms. Juan Min).

Author contributions RS, LMG, and CL designed the experiments; RS and YZ performed the experiments; RS, WH, YZ, LC, SSG, AHS, JY, LMG, and CL analyzed the data; RS, LMG, and CL wrote the paper.

Funding This work was supported in part by National Institutes of Health, National Heart, Lung, and Blood Institute (Grant R01-HL41178 to LMG), by MOST (2018YFA0507201 to CL), by the Strategic Priority Research Program A of the Chinese Academy of Sciences (XDA12010309 to CL), by the National Basic Research Priorities Program of China (2013CB911102 to CL), and by National Science Foundation of China (31670170 to CL).

Compliance with ethical standards

Conflict of interest The authors declare that they have no conflict of interest.

References

1. Prockop DJ, Kivirikko KI (1995) Collagens: molecular biology, diseases, and potentials for therapy. Annu Rev Biochem 64:403–434. https://doi.org/10.1146/annurev.bi.64.070195.002155
2. Cardinale GJ, Udenfriend S (1974) Prolyl hydroxylase. Adv Enzymol Relat Areas Mol Biol 41:245–300
3. Helaakoski T, Vuori K, Myllyla R, Kivirikko KI, Pihlajaniemi T (1989) Molecular cloning of the alpha-subunit of human prolyl 4-hydroxylase: the complete cDNA-derived amino acid sequence and evidence for alternative splicing of RNA transcripts. Proc Natl Acad Sci USA 86(12):4392–4396
4. Helaakoski T, Veijola J, Vuori K, Rehn M, Chow LT, Taillon-Miller P, Kivirikko KI, Pihlajaniemi T (1994) Structure and expression of the human gene for the alpha subunit of prolyl 4-hydroxylase. The two alternatively spliced types of mRNA correspond to two homologous exons the sequences of which are expressed in a variety of tissues. J Biol Chem 269(45):27847–27854

5. Annunen P, Helaakoski T, Myllyharju J, Veijola J, Pihlajaniemi T, Kivirikko KI (1997) Cloning of the human prolyl 4-hydroxylase alpha subunit isoform alpha(II) and characterization of the type II enzyme tetramer. The alpha(I) and alpha(II) subunits do not form a mixed alpha(I)alpha(II)beta2 tetramer. J Biol Chem 272(28):17342–17348
6. Kukkola L, Hieta R, Kivirikko KI, Myllyharju J (2003) Identification and characterization of a third human, rat, and mouse collagen prolyl 4-hydroxylase isoenzyme. J Biol Chem 278(48):47685–47693. https://doi.org/10.1074/jbc.M306806200
7. Gilkes DM, Bajpai S, Chaturvedi P, Wirtz D, Semenza GL (2013) Hypoxia-inducible factor 1 (HIF-1) promotes extracellular matrix remodeling under hypoxic conditions by inducing P4HA1, P4HA2, and PLOD2 expression in fibroblasts. J Biol Chem 288(15):10819–10829. https://doi.org/10.1074/jbc.M112.442939
8. Ruotsalainen H, Vanhatupa S, Tampio M, Sipila L, Valtavaara M, Myllyla R (2001) Complete genomic structure of mouse lysyl hydroxylase 2 and lysyl hydroxylase 3/collagen glucosyltransferase. Matrix Biol 20(2):137–146
9. Murad S, Sivarajah A, Pinnell SR (1980) Prolyl and lysyl hydroxylase activities of human skin fibroblasts: effect of donor age and ascorbate. J Invest Dermatol 75(5):404–407
10. Murad S, Sivarajah A, Pinnell SR (1981) Regulation of prolyl and lysyl hydroxylase activities in cultured human skin fibroblasts by ascorbic acid. Biochem Biophys Res Commun 101(3):868–875
11. Skropeta D (2009) The effect of individual N-glycans on enzyme activity. Bioorg Med Chem 17(7):2645–2653. https://doi.org/10.1016/j.bmc.2009.02.037
12. Kedersha NL, Tkacz JS, Berg RA (1985) Characterization of the oligosaccharides of prolyl hydroxylase, a microsomal glycoprotein. Biochemistry 24(21):5952–5960
13. Lamberg A, Pihlajaniemi T, Kivirikko KI (1995) Site-directed mutagenesis of the alpha subunit of human prolyl 4-hydroxylase. Identification of three histidine residues critical for catalytic activity. J Biol Chem 270(17):9926–9931
14. Uitto J, Dehm P, Prockop DJ (1972) Incorporation of *cis*-hydroxyproline into collagen by tendon cells. Failure of the intracellular collagen to assume a triple-helical conformation. Biochim Biophys Acta 278(3):601–605
15. Sasaki T, Majamaa K, Uitto J (1987) Reduction of collagen production in keloid fibroblast cultures by ethyl-3,4-dihydroxybenzoate. Inhibition of prolyl hydroxylase activity as a mechanism of action. J Biol Chem 262(19):9397–9403
16. Myllyharju J, Kivirikko KI (2001) Collagens and collagen-related diseases. Ann Med 33(1):7–21
17. Peterkofsky B (1991) Ascorbate requirement for hydroxylation and secretion of procollagen: relationship to inhibition of collagen synthesis in scurvy. Am J Clin Nutr 54(6 Suppl):1135s–1140s. https://doi.org/10.1093/ajcn/54.6.1135s
18. Kedersha NL, Tkacz JS, Berg RA (1985) Biosynthesis of prolyl hydroxylase: evidence for two separate dolichol-media pathways of glycosylation. Biochemistry 24(21):5960–5967
19. Kelleher DJ, Karaoglu D, Mandon EC, Gilmore R (2003) Oligosaccharyltransferase isoforms that contain different catalytic STT3 subunits have distinct enzymatic properties. Mol Cell 12(1):101–111
20. Tuderman L, Myllyla R, Kivirikko KI (1977) Mechanism of the prolyl hydroxylase reaction. 1. Role of co-substrates. Eur J Biochem 80(2):341–348
21. Myllyla R, Tuderman L, Kivirikko KI (1977) Mechanism of the prolyl hydroxylase reaction. 2. Kinetic analysis of the reaction sequence. Eur J Biochem 80(2):349–357
22. Myllyla R, Kuutti-Savolainen ER, Kivirikko KI (1978) The role of ascorbate in the prolyl hydroxylase reaction. Biochem Biophys Res Commun 83(2):441–448
23. Puistola U, Turpeenniemi-Hujanen TM, Myllyla R, Kivirikko KI (1980) Studies on the lysyl hydroxylase reaction. II. Inhibition kinetics and the reaction mechanism. Biochim Biophys Acta 611(1):51–60
24. Puistola U, Turpeenniemi-Hujanen TM, Myllyla R, Kivirikko KI (1980) Studies on the lysyl hydroxylase reaction. I. Initial velocity kinetics and related aspects. Biochim Biophys Acta 611(1):40–50
25. Dalziel M, Crispin M, Scanlan CN, Zitzmann N, Dwek RA (2014) Emerging principles for the therapeutic exploitation of glycosylation. Science (New York, NY) 343(6166):1235681. https://doi.org/10.1126/science.1235681
26. Gao Z, Zhang H, Hu F, Yang L, Yang X, Zhu Y, Sy MS, Li C (2016) Glycan-deficient PrP stimulates VEGFR2 signaling via glycosaminoglycan. Cell Signal 28(6):652–662. https://doi.org/10.1016/j.cellsig.2016.03.010
27. Cherepanova NA, Gilmore R (2016) Mammalian cells lacking either the cotranslational or posttranslocational oligosaccharyltransferase complex display substrate-dependent defects in asparagine linked glycosylation. Sci Rep 6:20946. https://doi.org/10.1038/srep20946
28. Ruiz-Canada C, Kelleher DJ, Gilmore R (2009) Cotranslational and posttranslational N-glycosylation of polypeptides by distinct mammalian OST isoforms. Cell 136(2):272–283. https://doi.org/10.1016/j.cell.2008.11.047
29. Ueno T, Tanaka K, Kaneko K, Taga Y, Sata T, Irie S, Hattori S, Ogawa-Goto K (2010) Enhancement of procollagen biosynthesis by p180 through augmented ribosome association on the endoplasmic reticulum in response to stimulated secretion. J Biol Chem 285(39):29941–29950. https://doi.org/10.1074/jbc.M109.094607